

Hiroshi Kimura
Tsuneo Okubo

Rheological properties of sodium montmorillonite in exhaustively deionized dispersions and in the presence of sodium chloride

Received: 16 May 2001
Accepted: 31 October 2001
Published online: 30 March 2002
© Springer-Verlag 2002

H. Kimura · T. Okubo (✉)
Department of Applied Chemistry
Faculty of Engineering
Gifu University, Yanagido 1-1
Gifu 501-1193, Japan
E-mail: okubotsu@apchem.gifu-u.ac.jp
Fax: +81-58-2932628

Abstract The rheological properties of sodium montmorillonite particles were studied in exhaustively deionized aqueous dispersions and in the presence of a small amount of sodium chloride. The shear viscosities were several magnitudes higher than those expected from Einstein's coefficient and decreased sharply when the concentration of sodium chloride increased. The storage moduli of deionized dispersions were constant, irrespective of the angular frequency,

whereas they decreased sharply when the salt concentration and the angular frequency increased. The phase of the deionized dispersion was "solid" and transformed into "liquid" on the addition of sodium chloride.

Keywords Rheological properties · Sodium montmorillonite particles · Deionization · Sodium chloride · Debye screening length

Introduction

Counterions of colloidal particles in aqueous dispersions in the diffuse region are distributed according to the balance between thermal diffusion and electrical attraction. When the dispersion is exhaustively deionized with mixed-bed ion-exchange resins, the electrical double layer expands and the particles show a solidlike structure and even crystal-like behavior especially for monodisperse particles [1, 2, 3, 4, 5, 6, 7, 8, 9, 10, 11, 12, 13]; the colloidal dispersion changes from "liquid" to "solid" (or "crystal-like") in the course of the deionization.

Recently, mixed-ion-exchange resins have become available commercially; these can eliminate ionic impurities very effectively and completely from colloidal dispersions to levels as low as 2×10^{-7} M (due to only H^+ and OH^- from the dissociation of water). When colloidal particles are deionized as completely as possible by co-existing ion-exchange resins for more than 1 year, the resulting dispersion contains a very small number of ionic species, i.e., counterions from the dissociating groups of the particles and H^+ and OH^- ions from the dissociation of water. In the deionized state, various distinct

extraordinary properties are expected to occur as mentioned earlier, since the Debye length for the completely deionized dispersion is of the order of micrometers.

We have measured the viscosities of colloidal dispersions in the deionized ("salt-free") state with the use of an Ostwald-type viscometer and a rotational viscometer [14, 15, 16, 17, 18, 19]. Several extraordinary properties have been observed:

1. The reduced viscosity (specific viscosity, η_{sp} , divided by the sphere concentration, c) of liquidlike dispersions was much higher than that expected from Einstein's prediction and decreased sharply when NaCl was added [14, 15].
2. A sharp peak was observed in the reduced viscosity-concentration curves, which showed the phase transition between "liquid" and "solid" (or "crystal") structures [14, 15], and the concentration dependence of the reduced viscosity of the deionized dispersions was sensitive to the kind of colloidal particles [16, 17].
3. A sharp increase in the shear stress was observed when the shear strain increased for the crystal-like dispersions, and the elastic modulus was evaluated from this [18].

4. $\log \eta$ of the crystal-like dispersions increased linearly as $\log \dot{\gamma}$ (shear rate) decreased with a slope of -1 [18].
5. The absolute values of the viscosity of the deionized dispersions were highly sensitive to the ionic impurities [19].

In this work, we report the rheological properties of sodium montmorillonite dispersions deionized exhaustively for more than 8 years.

Experimental

Materials

Aqueous dispersions of sodium montmorillonite particles ($2.3 \pm 1.0 \mu\text{m}$ in diameter from the metallurgical microscope, Wako Pure Chemical Industries, Tokyo, lot no. M4M7304) were used. The dispersions were deionized for more than 8 years with coexistence of the mixed-bed cation- and anion-exchange resins [AG501-X8 (D), 20–50 mesh, Bio-Rad, Richmond, Calif.]. The concentration of the deionized dispersions ranged from 0.0047 to 0.0196 in volume fractions, ϕ , and the concentration of sodium chloride (Wako Pure Chemical Industries, Tokyo) from 1.0×10^{-6} to $1.0 \times 10^{-4} \text{ mol l}^{-1}$. The water used for the purification and for dispersion preparation was purified by a Milli-Q reagent grade system (Milli-RO5 plus and Milli-Q plus, Millipore, Co., Bedford, Mass.).

Rheological measurements

A coaxial type rheometer (Rheosol-G2000W-GF, UBM Co. Kyoto) was used for the measurements. Before the measurements, all the parts of the cells of the rheometer were rinsed with deionized water exhaustively as possible. In order to prevent pollution from carbon dioxide in air during the measurements, the experiment was completed within 6 h after the sample had been set into the cell. In the measurements of the stress-strain curve, the shear rates increased linearly from the equilibrium state at the increasing rates, $d\dot{\gamma}/dt$, of 1.8×10^{-6} , 1.8×10^{-5} and $1.8 \times 10^{-4} \text{ s}^{-2}$, and each were kept for 1,000 s. In the measurements of the steady-shear flow, the shear rates changed from 0.01 to 100 s^{-1} . In the dynamic measurements, the angular frequencies varied from 0.1 to 10 s^{-1} . The inner cylinder was 22 mm in diameter and 30 mm in height and the outer cup was 65 mm in height, and the gap was 1.5 mm. The strains applied to the sample were estimated as the true strain by subtracting the rotation of the inner cylinder from that of the outer cup. The torque was determined from the twist angle of the torsion wire of 0.5-mm diameter. The resolution of the torque sensor was in the range from 10^{-5} to 10^{-3} kgfm . All the measurements were made at 25°C .

Closeup observation and reflection spectroscopy

Photographing of the sodium montmorillonite dispersions in a test tube was made with a digital HD microscope (VH-7000, Keyence Co. Osaka). The reflection spectra of the colloidal samples at an incident angle of 90° were recorded through the wall of the observation cell using a photonic multichannel analyzer (MCPD-7000, Otsuka Electronics Co., Osaka) connected to a Y-type optical-fiber cable.

Results and discussion

Closeup observation with a charge-coupled-device camera and reflection spectroscopy

Pictures of the dispersions were taken at a volume fraction of 0.0114 in the presence of ion-exchange resins. Single crystals were not recognized with the naked eye. This is due to the fact that the montmorillonite particles used here were highly polydisperse and the dispersion structure is solidlike amorphous. Reflection spectra were measured for the dispersions in the presence of ion-exchange resins. Very broad reflection peaks appeared in the dispersions irrespective of the particle concentration. This suggests a solidlike, amorphous character of the dispersion.

Stress-strain curves

The shear stress, σ , of the dispersions is shown in Fig. 1 as a function of strain, γ , increasing from 0 to 2.5. At a volume fraction, ϕ , of 0.0114, the shear stress increased linearly when the strain increased from 0 to 0.3. This observation suggests that the dispersion behaves as an elastic solid. From the slope, the elastic modulus at $\phi = 0.0114$ was estimated to be about 7.0 Pa. This dispersion showed yielding at $\gamma = 0.3$. When γ was larger than 0.3, the dispersion flowed and the shear stress approached 2.0 Pa. This observation suggests a liquidlike

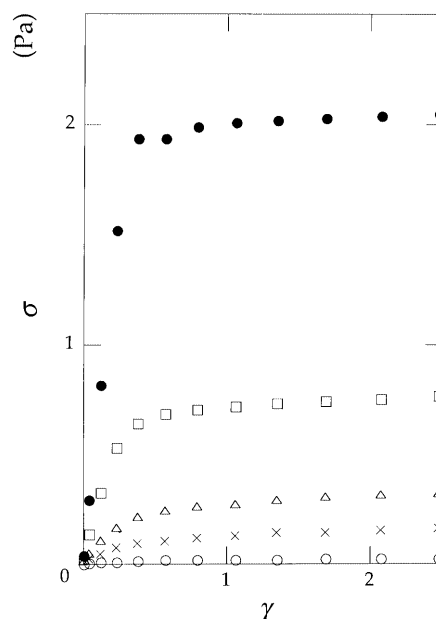


Fig. 1 Shear stress, σ , of a montmorillonite suspension as a function of the strain, γ , at 25°C . $\phi = 0.0055$ (open circles), 0.0068 (crosses), 0.0075 (triangles), 0.0086 (squares), 0.0114 (filled circles). $d\dot{\gamma}/dt = 1.8 \times 10^{-4} \text{ s}^{-2}$

nature for γ from 0.3 to 2.5. When the volume fraction of the particle was lower than 0.0075, a yielding strain was not clearly observed.

Plots of the σ values of the dispersions are shown in Figs. 2 and 3 as a function of the shear rate, $\dot{\gamma}$, in the startup flow when the shear rate increased up to 0.01 s^{-1} and at $\phi = 0.0068$ and 0.0114 , respectively. At $\dot{\gamma} = 0.01 \text{ s}^{-1}$, $d\dot{\gamma}/dt$ was $1.8 \times 10^{-4} \text{ s}^{-2}$, which corresponds to about half of the strain. It should be noted here that the shear stress increased linearly when the shear rate increased (Fig. 2). This observation supports the fact that the dispersion structure is “liquid”. On the other hand, at $\phi = 0.0114$, σ increased with the shear rate. The slopes varied depending on the values of the increasing rate, $d\dot{\gamma}/dt$, which means the dispersion at $\phi = 0.0114$ is solidlike amorphous.

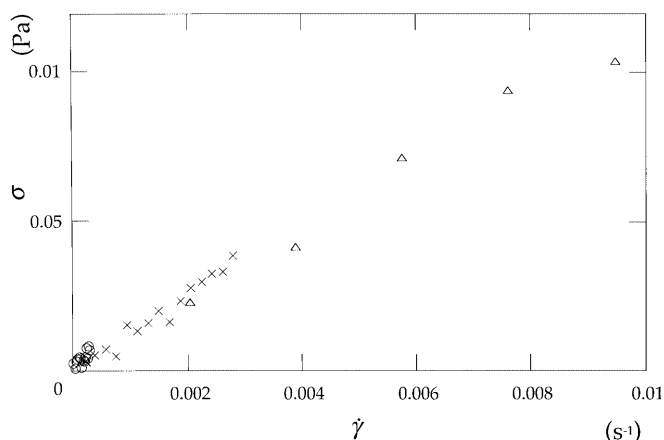


Fig. 2 σ of a montmorillonite suspension as a function of the shear rate, $\dot{\gamma}$, in the startup flow at 25°C . $\phi = 0.0068$. $d\dot{\gamma}/dt = 1.8 \times 10^{-6} \text{ s}^{-2}$ (circles), $1.8 \times 10^{-5} \text{ s}^{-2}$ (crosses), $1.8 \times 10^{-4} \text{ s}^{-2}$ (triangles)

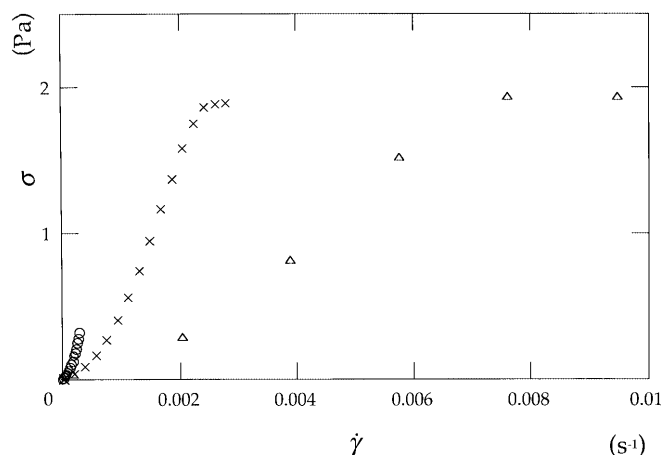


Fig. 3 σ of a montmorillonite suspension as a function of $\dot{\gamma}$ in the startup flow at 25°C . $\phi = 0.0114$. $d\dot{\gamma}/dt = 1.8 \times 10^{-6} \text{ s}^{-2}$ (circles), $1.8 \times 10^{-5} \text{ s}^{-2}$ (crosses), $1.8 \times 10^{-4} \text{ s}^{-2}$ (triangles)

Steady-shear properties

Plots of σ as a function of $\dot{\gamma}$ are shown in Fig. 4 for various volume fractions. At high volume fractions ($\phi > 0.0114$), $\log \sigma$ was rather insensitive to the shear rate. This suggests that the dispersion structure is solidlike or crystal-like. The shear stress decreased quite sharply as the volume fraction decreased, and as the shear rate increased, which means the dispersions were liquidlike.

σ is shown as a function of $\dot{\gamma}$ at $\phi = 0.0114$ and in the presence of sodium chloride in Fig. 5. At low concentrations of sodium chloride, below 1×10^{-5}

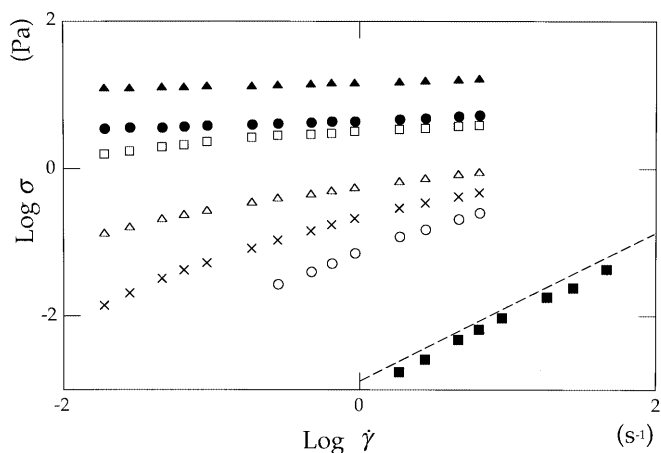


Fig. 4 σ of a montmorillonite suspension as a function of $\dot{\gamma}$ at 25°C . $\phi = 0.0046$ (open circles), 0.0054 (crosses), 0.0068 (open triangles), 0.0114 (open squares), 0.0139 (filled circles), 0.0196 (filled triangles). Water (filled squares). Broken line: prediction from Einstein's equation for $\phi = 0.0114$

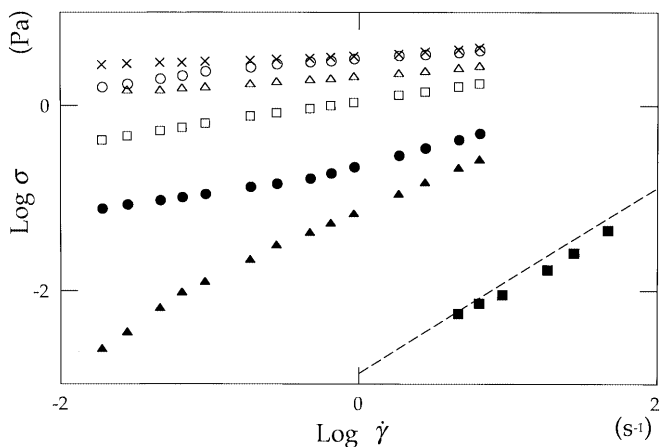


Fig. 5 σ of a montmorillonite suspension as a function of $\dot{\gamma}$ at 25°C . $\phi = 0.0114$. $[\text{NaCl}] = 0 \text{ mol l}^{-1}$ (open circles), $1 \times 10^{-6} \text{ mol l}^{-1}$ (crosses), $1 \times 10^{-5} \text{ mol l}^{-1}$ (open triangles), $3 \times 10^{-5} \text{ mol l}^{-1}$ (open squares), $7 \times 10^{-5} \text{ mol l}^{-1}$ (filled circles), $1 \times 10^{-4} \text{ mol l}^{-1}$ (filled triangles). Water (filled squares). Broken line: prediction from Einstein's equation for $\phi = 0.0114$

mol l⁻¹, the dispersion structure was solidlike, while it was liquidlike at higher salt concentrations. The shear viscosity, η , is shown as a function of the salt concentration in Fig. 6. A sharp decrease in the η values was observed when the salt concentration was higher than about 2×10^{-5} mol l⁻¹. This observation clearly suggests that the phase transition from a viscoelastic solid to a liquid occurs on the addition of sodium chloride.

According to the effective soft-sphere model, colloidal solidification may occur when the effective diameter of spheres including the electrical double layers, d_{eff} , is close to or larger than the intersphere distance, D [11]. When d_{eff} is close to or a slightly shorter than D , the dispersion structure is liquidlike. Gaslike dispersions are found when the effective size of the spheres is distinctly shorter than the intersphere distance. Here, the thickness of the electrical double layers is approximated roughly by the Debye screening length, D_1 [11]:

$$D_1 = (4\pi e^2 n / \epsilon k_B T)^{-1/2}, \quad (1)$$

where, e is the electronic charge, ϵ is the dielectric constant of the solvent, k_B is the Boltzmann constant. n is the concentration of “diffusible” or “free-state” cations and anions in dispersion. Thus, n is the sum of the concentrations of diffusible counterions, foreign salt and both H⁺ and OH⁻ from the dissociation of water.

The effective size of a sphere, d_{eff} , is given by the real diameter plus twice the Debye screening length, i.e., $d_0 + 2D_1$. When the dispersion is deionized exhaustively, the ionic concentration, c , becomes 2×10^{-7} mol l⁻¹, corresponding to the sum of H⁺ and OH⁻ ions from the dissociation of water. Thus the D_1 value in the deionized aqueous dispersion is estimated to be about 1 μm . On the addition of sodium chloride, c increases and then D_1 decreases. The phase transition from the solid to the liquid, therefore, occurs after the addition of sodium chloride.

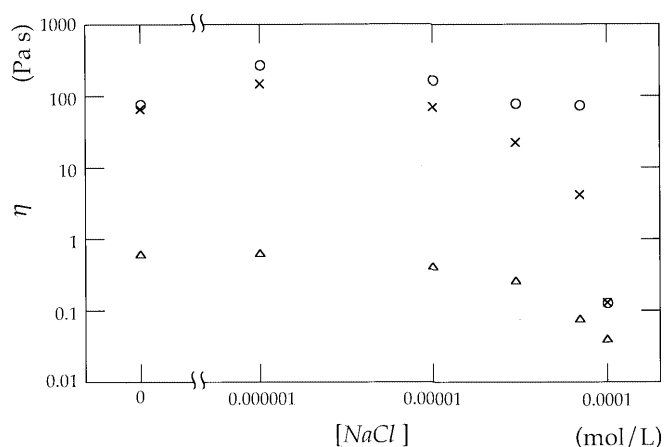


Fig. 6 Shear viscosity, η , of a montmorillonite suspension as a function of [NaCl] at 25 °C. $\phi = 0.0114$. $d\dot{\gamma}/dt = 1.8 \times 10^{-6} \text{ s}^{-2}$ (circles), $1.8 \times 10^{-5} \text{ s}^{-2}$ (crosses), $1.8 \times 10^{-4} \text{ s}^{-2}$ (triangles)

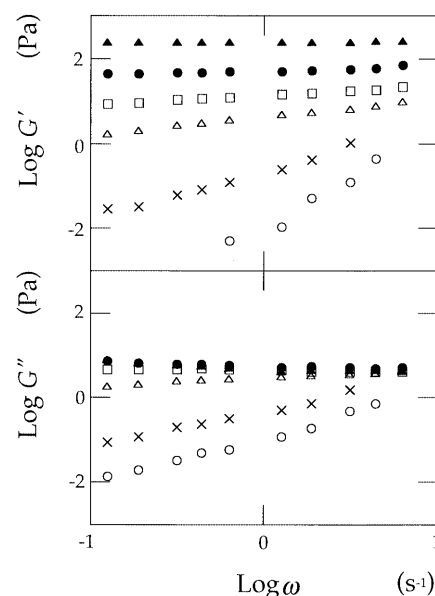


Fig. 7 Storage modulus, G' and loss modulus, G'' , of a montmorillonite suspension as a function of angular frequency, ω , at 25 °C. $\gamma = 0.02$. $\phi = 0.0047$ (open circles), 0.0055 (crosses), 0.0068 (open triangles), 0.0086 (squares), 0.0114 (filled circles), 0.0196 (filled triangles)

Dynamic shear properties

The storage modulus, G' , and the loss modulus, G'' , are shown in Fig. 7 as a function of the angular frequency, ω , at various volume fractions. At $\phi = 0.0114$ and 0.0196, G' was constant irrespective of ω . At $\phi \sim 0.01$, the dispersion showed a phase transition from a viscoelastic solid to a liquid. G estimated from the stress-strain relationship was 7.0 Pa at $\phi = 0.0114$ at $\gamma < 0.3$, which is smaller than the storage modulus, $G' \sim 40$, obtained from the dynamic measurements. The difference in the G and G' observed is due to the difference in the strains applied to the dispersion, i.e., γ is about 0.3 for the startup flow mode and about 0.02 for the dynamic shear mode. When γ is larger than about 0.1, structural changes, such as the sliding effect of the particles between the lattice planes and the change in the shape of the electrical double layers from spherical to flamelike, will occur as a result of the shearing forces [20]. Okubo [19] measured the elastic modulus, G , of dispersions, which had been deionized for 3 weeks, at $\phi = 0.13$ to be 0.12 Pa. This value is quite small compared with that of 7 Pa in this study. The reason for the difference is not clear yet; however, the difference in the time of the deionization process will be important. The profiles of G'' as a function of ω are similar to those of G' . G'' was larger than G' at $\phi < 0.0068$, and G'' was smaller than G' for $\phi > 0.0068$. Thus, the contribution from the elasticity corresponds with that from the viscosity increase with ϕ .

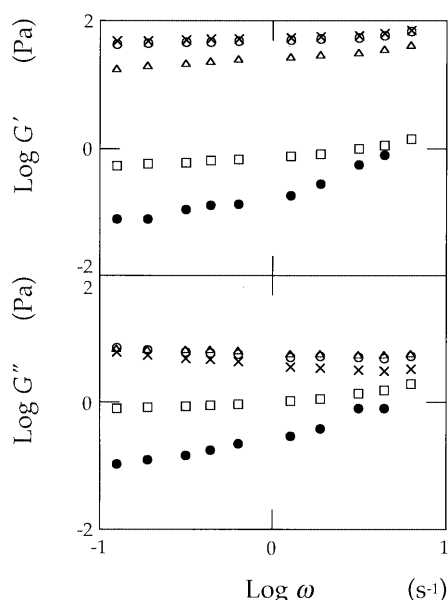


Fig. 8 G' and G'' of a montmorillonite suspension as a function of $[\text{NaCl}]$ at 25 °C. $\phi=0.0114$. $\gamma=0.02$. $[\text{NaCl}]=0 \text{ mol l}^{-1}$ (open circles), $1 \times 10^{-6} \text{ mol l}^{-1}$ (crosses), $1 \times 10^{-5} \text{ mol l}^{-1}$ (triangles), $7 \times 10^{-5} \text{ mol l}^{-1}$ (squares), $1 \times 10^{-4} \text{ mol l}^{-1}$ (filled circles)

G' is shown in Fig. 8 as a function of ω in the presence of sodium chloride again. A phase transition from solid to liquid on the addition of sodium chloride is observed. The order of magnitude of the elastic modulus of the colloidal dispersions is approximated by the magnitude of the thermal fluctuation, δ , of a sphere as [21]

$$G \sim f/D \sim (k_B T / \langle \delta^2 \rangle) / D, \quad (2)$$

where f is the force constant, D is the intersphere distance, δ is the thermal fluctuation of a sphere in the effective potential valley, and T is the temperature. By introducing a nondimensional parameter g for

$\langle \delta^2 \rangle > 1/2/D$, the modulus is obtained as a linear function of the number density of the spheres, N :

$$G \sim N k_B T / g^2. \quad (3)$$

When $g=1$, Eq. (3) gives the elastic modulus of an ideal gas having the same particle concentration. Lindemann's law of crystal melting tells us that $g < 0.1$ holds for the stable crystal. The g values evaluated in this work were 0.017 and 0.00018 at $\phi=0.0047$ and 0.0114, respectively. Clearly, the g value decreased when the particle concentration increased. It is highly plausible that the g values in the flowing state are larger than in the suspensions without shearing forces, since all the particles fluctuate largely by the shearing forces in the flow state.

Conclusion

Without NaCl, the storage modulus remained constant, irrespective of the angular frequency. Thus, the sodium montmorillonite dispersion behavior is solidlike amorphous as a result of the extended electric double layers around the particles in the exhaustively deionized suspension. With a small amount of NaCl (below $7 \times 10^{-5} \text{ mol l}^{-1}$), the dispersions remained solidlike, while G' decreased gradually as the concentration of NaCl increased. In the presence of a large amount of NaCl (above $1 \times 10^{-4} \text{ mol l}^{-1}$), G' decreased further, and $\log G'$ increased with $\log \omega$. These observations suggest that the dispersion structure transforms from a viscoelastic solid into a liquid state.

Acknowledgements The rheometer was purchased by Grants-in-Aid for Scientific Research on Priority Areas A (11167241) from the Japanese Ministry of Education, Science, Sports and Culture and Izumi Science and Technology Foundation, whom the authors thank greatly.

References

- Vanderhoff W, van de Hul HJ, Tausk RJM, Overbeek JThG (1970) In: Goldfinger G (ed) Clean surfaces: their preparation and characterization for interfacial studies. Dekker, New York, pp 15–44
- Hiltner PA, Papir YS, Krieger IM (1971) J Phys Chem 75:1881
- Kose A, Ozaki M, Takano K, Kobayashi Y, Hachisu S (1973) J Colloid Interface Sci 44:330
- Williams R, Crandall RS, Wojtowicz PJ (1976) Phys Rev Lett 37:348
- Mitaku S, Ohtsuki T, Enari K, Kishimoto A, Okano K (1978) Jpn J Appl Phys 17:305
- Lindsay HM, Chaikin PM (1982) J Chem Phys 76:3774
- Pieranski P (1983) Contemp Phys 24:25
- Ottewill RH (1985) Ber Bunsenges Phys Chem 89:517
- Aastuen DJW, Clark NA, Cotter LK, Ackerson BJ (1986) Phys Rev Lett 57:1733
- Pusey PN, van Megen W (1986) Nature 320:340
- Okubo T (1988) Acc Chem Res 21:281
- Russel WB, Saville DA, Schowalter WR (1989) Colloidal dispersions. Cambridge University Press, Cambridge
- Sood AK (1991) Solid State Phys 45:2
- Okubo T (1987) J Chem Phys 87:6733
- Okubo T (1988) Naturwissenschaften 75:91
- Okubo T (1988) Polym Bull 20:269
- Okubo T, Takezawa K, Kimura H (2000) Colloid Polym Sci 278:571
- Okubo T (1988) Ber Bunsenges Phys Chem 92:504
- Okubo T (1990) Colloid Polym Sci 268:1159
- Okubo T, Kimura H, Hatta T, Kawai T (2002) Phys Chem Chem Phys (in press)
- Mitaku S, Ohtsuki T, Okano K (1980) Jpn J Appl Phys 19:439